A Study of the Intermetallic Compounds of Gold and Manganese through the Use of the ^{197}Au Mössbauer Effect at 4.2°K and as a Function of Pressure*

David O. Patterson,† J. O. Thomson‡
Oak Ridge National Laboratory, Oak Ridge, Tennessee

and
University of Tennessee, Knoxville, Tennessee

and

P. G. Huray,‡ and Louis D. Roberts§
Oak Ridge National Laboratory, Oak Ridge, Tennessee and University of Tennessee, Knoxville, Tennessee
and
University of North Carolina, Chapel Hill, North Carolina
(Received 26 May 1969; revised manuscript received 2 June 1970)

The Mössbauer spectra of the ^{197}Au nuclei in Au, Au_4Mn, Au_3Mn, Au_2Mn, AuMn, $AuMn_3$, and dilute alloys of Au in Mn have been measured at 4.2°K. The isomer shift, magnetic dipole, and electric quadrupole splittings observed for these alloys are discussed in terms of the magnetic and crystalline structure. In these ordered gold-manganese alloys, the isomer shift as a function of composition departs widely from the linearity often observed for gold solid-solution alloys. For Au_2Mn, we find an effective field at the ^{197}Au nucleus of 1590 kG as well as a large quadrupole coupling. The spectrum we observe for Au_2Mn is consistent with the helical magnetic structure generally assumed for this alloy. A detailed analysis of this spectrum gives the magnetic moment $\mu^* = 0.415 \pm 0.004\ \mu_N$ for the 77.345-keV state of ^{197}Au, subject to a correction for the hyperfine-structure anomaly. For Au_2Mn, Mössbauer measurements have also been made as a function of pressure between 0 and 46 kbars. A 7% increase in the magnitude of the effective field at the ^{197}Au nucleus is observed between 0 and 30 kbar. This may be due to the uncoiling of the Mn spin helix observed by other workers in this pressure range.

I. INTRODUCTION

Gold and manganese form a series of intermetallic compounds which have been studied extensively through the use of neutron,[1-3] electron,[4] and x-ray[5-8] diffraction techniques, by magnetic[9-14] and electrical resistance measurements,[9,11] and by high-pressure methods.[3,9,12,13] These studies primarily give information about the crystalline and magnetic structure of the alloy, and about the magnetic moments of the manganese atoms. In this earlier work, comparatively little was learned about the properties of the nonmagnetic element, gold, in these compounds.

In this paper we give the results of a survey of the hyperfine-structure (hfs) coupling to the ^{197}Au nucleus in five manganese-gold intermetallic compounds and in 0.3 and 1 at.% of Au in Mn. These measurements were made through the use of the Mössbauer effect[15] for ^{197}Au.

Numerous earlier studies of the ^{197}Au Mössbauer effect have been made, for example, by Nagle *et al.*,[16] Shirley *et al.*,[17-19] Faltens,[20] Cohen *et al.*,[21,22] and by ourselves. In our earlier studies, we have measured the Mössbauer effect for gold alloys where the gold was in solid solution[23-25] and for the ordered and disordered phases of the copper-gold alloy system.[26] In this present work, by contrast, we study an alloy system characterized by highly ordered intermetallic compounds. Some aspects of the work have been reported previously.[27,28]

In a correlative study,[29] the low-temperature group of the University of Southampton, England, has measured the electronic and total nuclear specific heats of these Au-Mn alloys. The ^{197}Au Mössbauer hfs measurements reported here enable one to calculate the contribution of gold to the nuclear specific heat. When this is subtracted from the total nuclear specific heat, the specific-heat contribution due to the manganese hfs coupling may be obtained.

The Mössbauer hfs spectra of ^{197}Au for these alloys may be described by the spin Hamiltonian for the first excited state $\tilde{\mathcal{H}}^*$, and that for the ground state $\tilde{\mathcal{H}}$, where

$$\tilde{\mathcal{H}}^* = \Delta E_I + \tilde{\mathcal{H}}_M^* , \tag{1a}$$

$$\tilde{\mathcal{H}} = \tilde{\mathcal{H}}_M + \tilde{\mathcal{H}}_Q . \tag{1b}$$

ΔE_I is the measured isomer shift[30] between the absorber and the source, and is given by

$$\Delta E_I = B(\overline{P}_{\text{alloy}} - \overline{P}_{\text{source}}), \tag{2a}$$

where

$$\bar{P}_{\text{alloy}} = |\psi_a(0)|^2 / |\psi_{\text{Au}}(0)|^2 , \quad (2b)$$

$$\bar{P}_{\text{source}} = |\psi_s(0)|^2 / |\psi_{\text{Au}}(0)|^2 , \quad (2c)$$

$$B = K|\psi_{\text{Au}}(0)|^2 \delta r_n / r_n . \quad (2d)$$

K is a calculable constant, and δr_n is the difference in the values for the nuclear radius r_n between the excited and ground states of the gold nucleus. $|\psi_i(0)|^2$ is the electron charge density at the gold nucleus and the subscript i indicates the environment of the gold atom, Au for pure gold, a for gold in an alloy, and s for gold in the source of the Mössbauer radiation. In two previous studies[23,31] we have obtained a value for B of 8 ± 1 mm/sec.[32] For this value for B and with ΔE_I for metallic gold, Table II, $\bar{P}_s = 1.153$ for our platinum source (see below).

$\tilde{\mathcal{H}}_M$ describes the interaction of the ground-state nuclear magnetic moment μ with the alloy electrons in terms of an effective magnetic field H, and is given by

$$\tilde{\mathcal{H}}_M = -(\mu/I) H \tilde{I}_z . \quad (3a)$$

I is the nuclear spin of the ground state and $\tilde{I}_z$ is the z component of the nuclear spin operator. For ^{197}Au, $\mu = 0.144\,86 \pm 0.000\,07\ \mu_N$[33] and $I = \frac{3}{2}$. A similar Hamiltonian $\tilde{\mathcal{H}}_M^*$ applies to the first excited state,

$$\tilde{\mathcal{H}}_M^* = -[\mu^*(1+\epsilon)/I^*] H \tilde{I}_z^* . \quad (3b)$$

Here, the nuclear spin $I^* = \frac{1}{2}$. The factor $(1+\epsilon)$ describes the Bohr-Weisskopf effect[34] or hfs anomaly.[35] μ^* is the excited-state magnetic moment, and $\tilde{I}_z^*$ is the z component of the nuclear-spin operator for the excited state. Cohen[21] has given a value for $\mu^*(1+\epsilon) = 0.419 \pm 0.005 \mu_N$ from a study of dilute solutions of gold in iron using the Mössbauer effect. This value is in agreement with earlier Mössbauer determinations made on ^{197}Au dissolved in Fe, Co, and Ni.[19,24,28,36]

In Eq. (1b), $\tilde{\mathcal{H}}_Q$ is the interaction in the spin-$\frac{3}{2}$ ground state between the nuclear electric quadrupole moment[37] of 0.56 b for ^{197}Au and the electric field gradient (efg) at the ^{197}Au nucleus. For the interpretation of our results for Au_2Mn, we have assumed that the Au nuclei are situated in an axially symmetric efg with symmetry axis perpendicular to the effective magnetic field H. In this case,

$$\tilde{\mathcal{H}}_Q = \tfrac{1}{2} P[3\tilde{I}_x^2 - I(I+1)] , \quad (4)$$

where P is the quadrupole coupling constant, and H is assumed to lie along the z axis. For this case the nuclear state vectors are not eigenfunctions of $\tilde{I}_z$ alone. A study of the eigenvalues of the Hamiltonian, Eq. (1b), has been made by Parker.[38]

The observed lines in the Mössbauer spectra result from transitions between eigenstates of $\tilde{\mathcal{H}}^*$ and $\tilde{\mathcal{H}}$. The 77.345-keV state in ^{197}Au decays by means of a mixture of $M1$ and $E2$ radiation with a ratio of intensities $E2/(M1+E2) = 0.10 \pm 0.01$.[17] Thus, transitions for which $\Delta m = 0, \pm 1, \pm 2$ are observed, where Δm is the change in the z projection quantum number of the nuclear spin.

In the case of a pure Zeeman splitting of the nuclear states, Eqs. (3), and with $E2/(M1+E2) = 0.10$,[17] the Mössbauer spectrum will consist of eight lines with the sequence of relative intensities 2.0, 9.0, 16.0, 23.0, 23.0, 16.0, 9.0, and 2.0. If the Hamiltonian, Eq. (1b), includes both $\mathcal{H}_M$ and the $\mathcal{H}_Q$ of Eq. (4), these intensities will be altered somewhat. This will be discussed below in connection with the results for the alloy Au_2Mn.

For the full interpretation of our Mössbauer spectra, the natural linewidth of the transition Γ must be known. In another study[39] we have obtained a value of $\Gamma = 0.923 \pm 0.006$ mm/sec. The corresponding "thin sample" linewidth which appears in Mössbauer measurements is 2Γ. Our result agrees with that of Steiner *et al.*[40] who give the value $\Gamma = 0.935 \pm 0.007$ mm/sec.

The nuclear specific heat C_n is given in terms of the nuclear ground-state Hamiltonian, Eq. (1b), as

$$C_N = dE_n/dT , \quad (5a)$$

where

$$E_n = \mathrm{Tr}\,\tilde{\mathcal{H}} e^{-\tilde{\mathcal{H}}/kT} / \mathrm{Tr}\, e^{-\tilde{\mathcal{H}}/kT} . \quad (5b)$$

If both magnetic hfs, Eq. (3a), and electric quadrupole hfs, Eq. (4), are present, then C_n is given to terms in T^{-3} by

$$C_n T^2/R \cong \alpha H^2 + \beta P^2 + \gamma_\perp H^2 P/kT , \quad (5c)$$

where R is the gas constant and where

$$\alpha = (\mu/I)^2 I(I+1)/3k^2 ,$$

$$\beta = I(I+1)(2I-1)(2I+3)/20k^2 ,$$

$$\gamma_\perp = +(\mu/I)^2 I(I+1)(2I-1)(2I+3)/20k^2 .$$

T is the absolute temperature and k is the Boltzmann constant. $\gamma_\perp$ corresponds to the case assumed here for which the magnetic and quadrupole coupling axes are at an angle of $\frac{1}{2}\pi$.

II. EXPERIMENTAL DETAILS

The Mössbauer spectrometer used for this work was in many ways similar to a high-pressure Mössbauer apparatus described in some detail previously.[31] Like this high-pressure equipment, it consisted of a liquid-helium temperature cryostat and a sine-wave transducer used in conjunction with a multichannel analyzer operating in the pulse-height mode. The transducer armature extended from the liquid-helium temperature region of the

TABLE I. Alloy sample preparation. With the exception of the 1%-Au alloy, the sample constituents were melted and the resulting alloys were homogenized prior to cutting into appropriately shaped specimens. The samples were then given an ordering anneal somewhat below the temperature at which the ordering takes place. X-ray analyses were carried out on all samples, and chemical analyses were performed on most of the samples.

Alloy	Anneal Temp. (°C)	Time (h)	X-ray Analysis [a]
0.3% Au in Mn	685–689	72	~100% α-Mn phase
1% Au in Mn	quenched from melt		~98% α-Mn phase Remainder probably $AuMn_3$
$AuMn_3$ 24.76-at.% Au	640–655	100	~95% $AuMn_3$ Remainder probably γ-Mn $a=4.715$; $c=2.848$
AuMn 50.00-at.% Au	575–585	100	~100% β_2-AuMn $a=3.163$; $c=3.302$
Au_2Mn *A* 66.07-at.% Au	670–700	100	~98% Au_2Mn ~2% Au_3Mn
Au_2Mn *B*	700	100	~100% Au_2Mn
Au_3Mn 75.19-at.% Au	610–622	100	~90–100% Au_3Mn plus some unidentified phase
Au_4Mn	800	50	~100% Au_4Mn [b]
	350	70	
	250–300	10	

[a] Limit of x-ray detection of impurity phases is ~2%.
[b] Metallographic examination revealed ~1% of an impurity phase.

cryostat to the room-temperature region. To monitor and to reduce the effects of any slight drift of linearity or gain of the analyzer and associated electronic equipment, a six-line Mössbauer iron reference spectrum and the gold Mössbauer spectrum were taken simultaneously using the same transducer and electronic equipment. The reference six-line iron spectrum was taken with the iron absorber foil at room temperature (299 ± 3) °K, with the ^{57}Co in Cu source mounted on the transducer armature. The gold γ-ray source was a 200-mg sample of Pt enriched to 65% in ^{196}Pt which was neutron activated in the Oak Ridge Research Reactor. This was mounted at the liquid-helium temperature end of the transducer armature and the Au-Mn alloy Mössbauer absorber was also at 4.2 °K. Both the Fe and the Au spectra were spread over about 400 analyzer channels. About 5×10^5 counts/channel were taken in a gold spectrum and ~10^5 counts/channel were taken in an iron Mössbauer spectrum. In a typical gold spectrum the maximum Mössbauer absorption was 4–10% and for a typical iron spectrum was about 18%.

Equations (1a) and (1b) have been fitted to the measured gold and iron spectra using a computer code developed by Czjzek of the Oak Ridge National Laboratory. This code gives a least-squares fit of a sum of lines of Lorentz shape to the experimental data. Using this code it is possible to impose any desired set of linear constraints between the linewidths, intensities, and positions of the lines so as to reduce the number of independent parameters which must be optimized for the fit. The code also computes an error for each independent parameter which reflects both the statistical errors in the data points and also the quality of the fit.[41] This is the error which is quoted with the results.

Except for the Au_2Mn spectra, where the method of fitting will be discussed below, the fits were performed as follows. All individual linewidth parameters were constrained to be equal and their common linewidth was one of the parameters to be determined. The relative line intensities given above were assumed. The values $\mu = 0.144\,86\,\mu_N$ and $\mu^*(1+\epsilon) = 0.420$, obtained from our earlier report on Au_2Mn, were used to constrain the ratio of the ground-state and excited-state splittings.

In Table I we have summarized the details of the preparation and the results of x-ray and chemical analyses of the gold alloy absorbers studied here.

III. RESULTS

In Table II, we list the values for the parameters obtained from computer fits of Eqs. (1a) and (1b) to the measured alloy spectra. We give below some additional comments about the measurements for each of the alloys, and a summary of the principal results obtained.

A. Au_4Mn

The ordered alloy Au_4Mn is ferromagnetic with a Curie temperature of 361 °K.[10] The Mössbauer absorption spectrum for ^{197}Au in Au_4Mn at 4.2 °K was a somewhat asymmetric doublet and could not quite be described by any simple Hamiltonian where all of the Au atoms were equivalent. The effective field determined from an estimate of the excited-state splitting was roughly 700 kG, and the center of gravity of the spectrum corresponded to an isomer shift of 0.15 ± 0.10 mm/sec, relative to the Au in Pt source. It is possible that the sample was not perfectly ordered, although our x-ray analysis showed only the presence of ordered Au_4Mn. A more complete study of Au_4Mn has been made recently by Cohen *et al.*[22]

B. Au_3Mn

The ordered alloy Au_3Mn is antiferromagnetic with a Néel temperature of 145 °K.[10] The Mössbauer absorption spectrum is a symmetric partially resolved doublet. The data could be fitted quite well assuming only a Zeeman splitting. However, for the sample thickness used, a linewidth which was unusually large in comparison with the other gold-manganese alloys was required for the fit. Some of this broadening may correspond to the fact that there are four inequivalent gold sites in the antiphase domain structure for

Au_3Mn.[4] The effective magnetic field given in Table II would then be the average value for the gold sites.

C. Au_2Mn

Ordered Au_2Mn crystallizes in a body-centered tetragonal structure[6,7] having sheets of Mn atoms parallel to the basal plane. These sheets are separated by two similar sheets of Au atoms. In zero magnetic field and at zero pressure, the Néel temperature is 363 °K. Neutron diffraction measurements at 77° and 300 °K are consistent with a helical antiferromagnetic structure.[1,3] In this proposed structure, the Mn magnetic moments in each sheet or layer are coupled ferromagnetically and lie in a direction perpendicular to the crystalline c axis. The direction of the layer moment turns by an angle Φ from Mn layer to Mn layer along the c axis. At 77 °K, $\Phi \cong 47°$ and at 300 °K, $\Phi \cong 51°$. The alloy appears to become ferromagnetically oriented, i.e., $\Phi = 0°$, under a pressure of 16 kbar at room temperature[13] or upon the application of a magnetic field H_c.[10] H_c increases from ~11 kG[10,14] at room temperature to ~15 kG at 4.2 °K.[14] The apparently continuous change of H_c with temperature suggests that the magnetic structure at 4.2 °K is also a helix similar to that observed at higher temperatures, but the structure has not been investigated by neutron diffraction methods at liquid-helium temperatures.

The Mössbauer spectrum for the 88-mg/cm^2 sample of Au_2Mn, Table II, is shown in Fig. 1. This figure has been published previously along with some of our earlier results for this alloy.[28] It is included as a typical example of our Mössbauer measurements reported here on the gold-manganese alloys. Some additional results for Au_2Mn are given below.

As may be seen from Fig. 1, the Au_2Mn Mössbauer spectrum consists of two well-separated groups of lines, and each of these groups consists of four lines which are partially resolved. The effects of both electric and magnetic hfs coupling are clearly shown by the spacing of the lines.

A theoretical treatment of line intensities appropriate for mixed dipole and quadrupole radiation between arbitrary nuclear states has been given by Karyagin.[42] From this formulation, with $PI/\mu H = 0.25$ (see Table II), with the assumption that the axis of $\tilde{H}_M$ and the principal axis of $\tilde{H}_Q$ are at an angle of $\frac{1}{2}\pi$, and with the ratio of intensities[17] $E2/(E2+M1) = 0.10$, the theoretical relative line intensities to be expected are 2.53, 9.43, 15.80, 23.13, 22.87, 15.98, 9.69, and 2.27 with increasing line

TABLE II. hfs coupling paramenters for ^{197}Au in ordered Au-Mn alloys measured by the Mössbauer effect at 4.2 °K. μ^* is the ^{197}Au excited-state magnetic moment; $(1+\epsilon)$ describes the hfs anomaly (Ref. 34); H is the effective magnetic field at the gold nucleus; P is the quadrupole coupling constant [Eq. (4)]; μ is the magnetic moment; and I is the nuclear-spin quantum number for the ground state of ^{197}Au. ΔE_I is the Mössbauer isomer shift of the absorber nuclei relative to an Au in Pt source and $\bar{P}_{\text{alloy}}$ is the ratio of the total valence electron probability density at gold absorber nuclei relative to pure gold. $\bar{P}_{\text{alloy}} = |\psi_{\text{alloy}}(0)|^2/|\psi_{\text{Au}}(0)|^2$. See text.

Alloy	$2\mu^*(1+\epsilon)H$ (mm/sec)	H[a] (kG)	$\lambda = \frac{PI}{\mu H}$	ΔE_I[b] Eq. (2) (mm/sec)	$\bar{P}_{\text{alloy}}$ Eq. (2)	Linewidth parameters (mm/sec)	Gold density (mg/cm^2)	Comments
0.3% Au in Mn	2.91±0.08	286±8		3.88±0.04	1.638	3.23±0.11	46	
1% Au in Mn	2.82±0.04	278±5		3.93±0.03	1.644	2.67±0.05	158	
$AuMn_3$	2.79±0.06	275±6		3.85±0.03	1.634	1.99±0.06	137	
AuMn				3.39±0.02	1.576	2.97±0.04	242	$\theta_D \sim 173$ °K
Au_2Mn-I	16.13±0.05	1589±16	−0.257±0.013[c]	1.59±0.02	1.351	2.06±0.04	88	Melt *B*
Au_2Mn-II	16.18±0.02	1594±16	−0.243±0.009[c]	1.55±0.02	1.346	2.15±0.03	176	
Au_2Mn-III	16.10±0.02	1586±15	−0.238±0.006[c]	1.56±0.02	1.348	2.15±0.02	285	Melt *A*
Au_2Mn	16.73±0.06	1649±17	−0.244±0.016[c]	1.62±0.03	1.353	2.17±0.05	176	Pressure = 15.4 kbars, Melt *B*
Au_2Mn	17.34±0.08	1708±18	−0.252±0.021[c]	1.68±0.03	1.363	2.35±0.07	176	Pressure = 31.1 kbars, Melt *B*
Au_3Mn	7.99±0.04	787±8		0.59±0.02	1.226	2.81±0.05	141	Both measurements made
	8.08±0.05	795±9		0.62±0.02	1.230	2.40±0.05	74	with same alloy sample
Au_4Mn	see text							
Au				−1.22±0.01	1.000	2.58±0.09	95	

[a]Calculated from the excited-state splitting and the value for $\mu^*(1+\epsilon) = 0.415 \pm 0.004$ found from the study of Au_2Mn.
[b]Measured with respect to a gold in platinum source, $\bar{P}_s = 1.153$. See text.
[c]The values for λ are calculated under the assumption that the efg and magnetic field are perpendicular. See text.

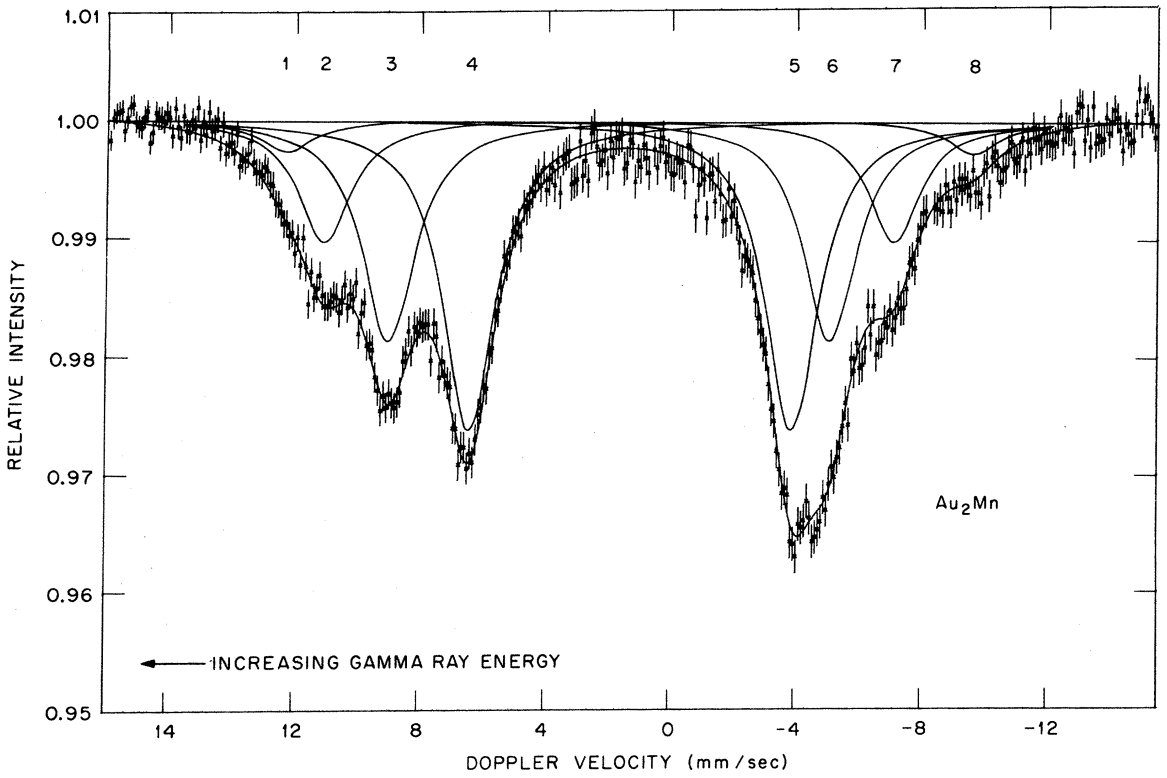

FIG. 1. Mössbauer absorption spectrum for ^{197}Au in Au_2Mn at 4.2 °K. The eight component lines and the curve through the data points were derived from the least-squares fit of the Hamiltonians, Eqs. (1), to the data.

energy. We have fitted our Au_2Mn data to the eigenvalues of the Hamiltonian [Eqs. (1), (3), and (4)] using these intensity ratios. From this fit, Fig. 1, we find that $\mu^*(1+\epsilon) = 0.415 \pm 0.004\ \mu_N$. This value agrees within error with the result in Ref. 28, where the first-order approximation that $I_1 = I_8$, $I_2 = I_7$, $I_3 = I_6$, and $I_4 = I_5$ was used.[43]

We see from Table II that the linewidth parameters observed for the three Au_2Mn samples at zero pressure are only slightly greater than the width $2\Gamma = 1.846$ mm/sec.[39] This observed width for Au_2Mn may be approximately accounted for in terms of thick absorber effects. This implies that the magnitude of the effective magnetic field is homogeneous throughout the sample to within our experimental error of about 1%.

Atoji[44] has recently observed that the neutron diffraction data taken on powder specimens of Au_2Mn could admit spin structures other than a helix. The magnetic structure must be one which will account for this sharp value for H which we observe. The helical structure which is usually assumed[1] for Au_2Mn does account for a sharp value of H and thus is consistent with our results.

The mean value found for the three samples for H, 1590 ± 15 kG, is the largest field observed thus far for ^{197}Au in magnetic materials. For the free gold atom in a strong external magnetic field, there is an effective field of 20.9×10^3 kG, corresponding to an hfs coupling of 6099.3 MHz.[33] Therefore, for Au in Au_2Mn, the effective field is $7\frac{1}{2}\%$ of that arising in the free atom through core polarization and directly from the unpaired 6s electron.

The quadrupole coupling constant P was found to be -0.48 ± 0.03 mm/sec or $-(1.00 \pm 0.06) \times 10^{-3}$ cm^{-1}. $\langle r^{-3} \rangle$ for a 5d hole on a free gold atom is $12.3/a_0^3$.[37] Thus about 0.17 of one 5d hole ($d_{x^2-y^2}$) is of a proper magnitude to describe the quadrupole coupling in Au_2Mn.

As we mentioned above, there is evidence that Au_2Mn becomes ferromagnetic at room temperature under an applied pressure between 10 and 20 kbar but no magnetic studies as a function of pressure have been made at 4.2 °K. We have obtained hfs spectra for Au_2Mn as a function of pressure to 46 kbar (see Ref. 28 and Table II). We find that H increases by about 7% between zero pressure and 30 kbar where within error the increase of H appears to saturate.

It is possible to describe this increase of H with

pressure in terms of the decrease of Φ for the Mn spin helix by the following simple model. We assume that the effective field at a given gold nucleus $\vec{H}$ is given by a vector sum of interactions of the Au with the oriented moments in nearby Mn planes. If $\hat{\mu}_i$ is a unit vector parallel to the magnetic moment of the atoms in the ith Mn plane, then we assume $\vec{H}=\sum_i a_i \hat{\mu}_i$ where the coefficients a_i give the strength at a gold nucleus of the field components from each Mn layer. We limit ourselves to only the nearest and next-nearest Mn planes to a given Au atom, $i=1, 2$. With Φ the spin rotation $a_1 \sin\alpha_1$ we define $=a_2 \sin\alpha_2$. $\alpha_1+\alpha_2=\Phi$. Then $H=(a_1 \cos\alpha_1+a_2\cos\alpha_2)$ and $a_1\sin\alpha_1 = a_2 \sin\alpha_2$. In the ferromagnetic state assumed to exist above 30 kbar, we find a maximum field $H_m=(a_1+a_2)$ for $\alpha_1=\alpha_2=\Phi=0$. Using $H_m/H \simeq 1.06$ and $\Phi=46°$, we find that

$$a_1/H_m=a_1/(a_1+a_2)\simeq 0.76 ,$$

$a_2/H_m \simeq 0.24$, and $\alpha_1 \simeq 10.6°$. It is plausible although not necessary to associate the stronger of these interactions a_1 with the nearer Mn plane at 1.46 Å.

D. AuMn

The ordered alloy AuMn is antiferromagnetic with a Néel temperature of approximately 520 °K.[10] Ordered AuMn has a tetragonally distorted CsCl structure.[8] The gold atoms are situated at the body-centered positions and lie between an antiferromagnetic arrangement of ferromagnetic sheets.[2] Because of this magnetic and crystallographic symmetry, the magnetic field at the gold nuclei is expected to be zero. Because of the near-cubic symmetry of the manganese atoms about the gold atoms, the efg at the gold nuclei may be zero or small.

The Mössbauer absorption spectrum for AuMn at 4.2 °K for a gold thickness of 242 mg/cm^2 consisted of a single line of width 2.97 ± 0.04 mm/sec. This width can be accounted for by thick absorber effects alone[39] if an effective Debye temperature of 173 °K is assumed for gold in the alloy.

E. $AuMn_3$

The ordered alloy $AuMn_3$ is antiferromagnetic with a Néel temperature of 903 °K.[10] The Mössbauer absorption spectrum for ^{197}Au in $AuMn_3$ showed only a partial resolution of the two unresolved ground-state quartets. An eight-line fit to this spectrum yielded an effective magnetic field at the gold nuclei in $AuMn_3$ of 275 ± 6 kG. The line-width parameter determined was 1.99 ± 0.66 mm/sec. The difference between this value and the natural width for metallic gold may be accounted for by thick absorber effects.

F. Dilute Gold in Manganese

It is evident from Table II that both the hfs splitting and the isomer shift for the two dilute alloy spectra are in agreement and are nearly the same as the values for these quantities obtained for the ordered $AuMn_3$. The principal difference in the spectra for the dilute alloys and ordered $AuMn_3$ is that substantially wider lines were required to fit the dilute alloy spectra, the greatest width occurring in the most dilute alloy. A possible explanation of these observations may be that, for these dilute alloys, there is a strong tendency for the gold atoms to cluster into small regions with compositions near $AuMn_3$. The large linewidths may then be associated with a fluctuation of the hfs coupling with cluster size or composition.

G. Isomer Shifts for Ordered Gold-Manganese Alloys

A plot of the isomer shifts for gold in the ordered gold-manganese alloys is shown in Fig. 2. These isomer shifts are positive with respect to metallic gold, implying through Eqs. (2) that

$$|\psi(0)|^2_{\text{alloy}}/|\psi(0)|^2_{\text{Au}}>1 .$$

Using our value[23,31] for B of 8 mm/sec, and ΔE_I from Table II, the value for this ratio for $AuMn_3$, for example, is ~1.6.

In Fig. 2, it may be seen that the gold isomer shift for the ordered gold-manganese alloys is not a linear function of composition. This is in contrast to the isomer shift for gold in solid solution in silver, for example, which is a highly linear function of composition.[23,26] It may be similar, however, to the isomer shift for gold in the copper-gold system[26] which is found to depend on short-range order. It is reasonable to suggest then that the nonlinear behavior of the gold isomer shift shown in Fig. 2 reflects not only atomic volume and composition, but also the specific crystalline structure of the alloys.

H. Nuclear Specific Heats

From the results of the hfs measurements on ^{197}Au we have calculated the contributions to CT^2/R from the gold in each of the ordered alloys and these contributions are given for reference in Table III. These values are used in the interpretation of low-temperature specific-heat measurements on these alloys by Lynam *et al.*[29]

IV. SUMMARY

We have studied the hfs coupling of the noble-metal component, gold, in a series of gold-man-

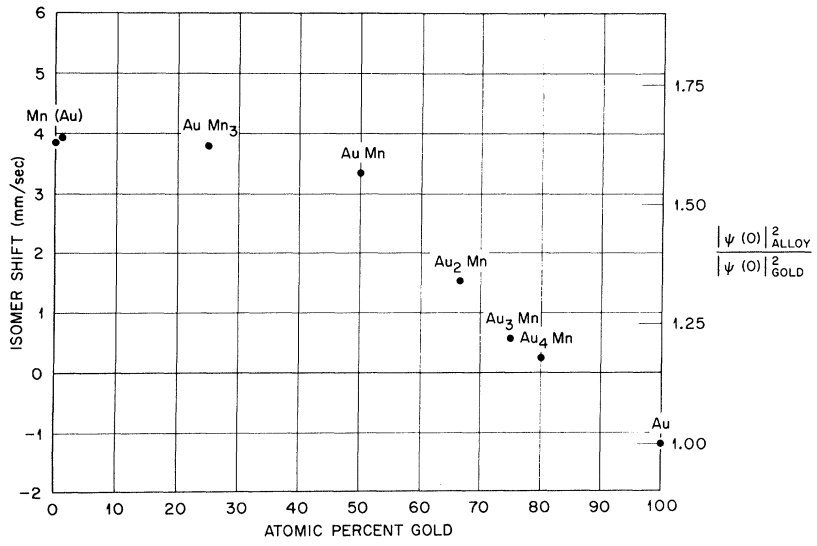

FIG. 2. Mössbauer isomer shift of gold as a function of concentration for ordered gold-manganese alloys. The right-hand scale gives

$$\bar{P} = |\psi_{\text{alloy}}(0)|^2 / |\psi_{\text{Au}}(0)|^2$$

calculated from Eq. (2). The errors are about $\frac{1}{2}$ of the diam of the plotted points. It is suggested that the nonlinear dependence of the isomer shift on concentration is related to the ordered structure of the alloy.

ganese intermetallic compounds. This hfs coupling was found to be consistent with available information about the crystal and magnetic structure of the alloys. In particular, the sharpness of the component lines in the observed hfs spectrum for ^{197}Au in Au_2Mn is consistent with a helical magnetic structure for that alloy. Because of the large value for H in the ordered alloy Au_2Mn, we have obtained a partially resolved hfs spectrum for ^{197}Au and have found that $\mu^*(1+\epsilon) = 0.415 \pm 0.004 \mu_N$. We have also obtained from the line intensities of the Au_2Mn spectrum an estimate of the $E2/(M1+E2)$ mixing ratio of 0.10 for the 77.345-keV γ ray which agrees with the value given by Shirley *et al.*[17] The close agreement between our value of $\mu^*(1+\epsilon)$ with that obtained by Cohen[21] for Au in Fe indicates that any difference in the gold hfs anomaly in Au_2Mn from that of Au in Fe is small.

We have measured the pressure dependence of the isomer shift, the quadrupole coupling, and the effective magnetic field for Au_2Mn. Our results for H may be described in terms of an increase of the effective magnetic field at a gold nucleus as the turn angle Φ of the Mn spin helix decreases with increasing pressure. The quadrupole coupling for Au in Au_2Mn is independent of pressure within our error of measurement. The increase of isomer shift with increasing pressure is similar to that found for metallic gold.[31]

A comparison of the spectra for the dilute alloys of Au in Mn with the spectrum of $AuMn_3$ suggests that there is a clustering of the Au atoms in the dilute alloys such that the immediate environment of the Au atom is similar to that found in $AuMn_3$.

The nonlinearity in the isomer shift as a function of composition for these ordered alloys is in contrast to the linear variation of isomer shift with concentration found in several gold solid-solution alloy systems.[23,24] It is analogous to that which has been observed in ordered gold-copper alloys.[26]

From the measured hfs we have calculated the contribution of the gold to the low-temperature specific heat of the alloys.

ACKNOWLEDGMENTS

We would like to thank Dr. R. G. Scurlock for giving us samples cut from the specimens used in their specific-heat measurements, and for helpful discussions. We are indebted to Dr. John Burton, Dr. D. A. Shirley, Dr. R. L. Cohen, and Dr. G. Hoy for helpful comments and discussions on various aspects of the paper.

TABLE III. Gold nuclear specific heat for ordered gold-manganese alloys as calculated using Eqs. (5) from the measured gold hfs coupling constants given in Table II.

Alloy	H_{Au} (kG)	(CT^2/R) (10^{-4} deg^2)
Au_4Mn	~ 700	0.080
Au_3Mn	791	0.097
Au_2Mn [a]	1590	0.440
AuMn	0	0
$AuMn_3$	275	0.012

[a] CT^2/R also contains the quadrupole coupling term using $P/k = 1.4 \times 10^{-3}$ deg. The term $\gamma_1 H^2 P/kT$ (Eq. 5) is negligible above 0.1 °K.

*Research jointly sponsored by the U. S. Atomic Energy Commission under contract with the Union Carbide Corp., and under contract AT-(40-1)-3897 with the University of North Carolina, by the University of Tennessee, and by the Advanced Research Projects Agency, Contract No. Sd100 at the University of North Carolina. This paper is based in part on a dissertation submitted by David O. Patterson to the Faculty of the University of Tennessee, Knoxville, Tenn., in partial fulfillment of the requirements for the Ph. D. degree in Physics.

†Oak Ridge Graduate Fellow from the University of Tennessee under appointment with Oak Ridge Associated Universities. Present address: Radiation Inc., P. O. Box 37, Melbourne, Fla.

‡Present address: Physics Department, University of Tennessee, Knoxville, Tenn.

§Present address: Physics Department, University of North Carolina, Chapel Hill, N. C.

[1]A. Herpin and P. Meriel, J. Phys. (Paris) 22, 337 (1961); A. Herpin, P. Meriel, and J. Villain, Compt. Rend. 249, 1334 (1959).

[2]G. E. Bacon, Proc. Phys. Soc. (London) 79, 938 (1962).

[3]F. A. Smith, C. C. Bradley, and G. E. Bacon, J. Phys. Chem. Solids 27, 925 (1966).

[4]D. Watanabe, J. Phys. Soc. Japan 15, 1030 (1960); 15, 1251 (1960).

[5]E. Raub, U. Zwicker, and H. Baur, Z. Metallk. 44, 312 (1953); A. Kussmann and E. Raub, *ibid.* 47, 9 (1956).

[6]J. H. Smith and R. Street, Proc. Phys. Soc. (London) B70, 1089 (1957).

[7]E. O. Hall and J. Royan, Acta Cryst. 12, 607 (1959).

[8]J. H. Smith and P. Gaunt, Acta Met. 9, 819 (1961).

[9]N. P. Grazhdankina and K. P. Rodionov, Zh. Eksperim. i Teor. Fiz. 43, 2024 (1962) [Soviet Phys. JETP 16, 1429 (1963)].

[10]A. J. P. Meyer and P. Taglang, J. Phys. Radium 17, 457 (1956); A. J. P. Meyer, J. Phys. (Paris) 20, 430 (1959).

[11]A. Giansoldati, J. O. Linde, and G. Borelius, J. Phys. Chem. Solids 9, 183 (1959).

[12]D. S. Rodbell, in *Progress in Very High Pressure Research*, edited by F. Bundy, W. R. Hibbard, and H. M. Strong (Wiley, New York, 1961), p. 285.

[13]R. C. Wayne and F. A. Smith, J. Chem. Phys. Solids 30, 183 (1969).

[14]T. Hirone, Appl. Phys. 36, 988 (1965); N. Kazama, T. Hirone, K. Kamigaki, and T. Kaneko, J. Phys. Soc. Japan 24, 980 (1968).

[15]R. L. Mossbauer, Z. Physik 151, 124 (1958); H. Frauenfelder, *The Mössbauer Effect* (Benjamin, New York, 1962).

[16]D. Nagle, P. P. Craig, J. G. Dash, and R. R. Reiswig, Phys. Rev. Letters 4, 237 (1960).

[17]D. A. Shirley, M. Kaplan, and P. Axel, Phys. Rev. 123, 816 (1961).

[18]P. H. Barrett, R. W. Grant, M. Kaplan, D. A. Keller, and D. A. Shirley, J. Chem. Phys. 39, 1035 (1963).

[19]R. W. Grant, M. Kaplan, D. A. Keller, and D. A. Shirley, Phys. Rev. 133, A1062 (1964).

[20]Faltens, thesis, University of California, Berkeley, 1969 (unpublished).

[21]R. L. Cohen, Phys. Rev. 171, 343 (1968).

[22]R. L. Cohen, J. H. Wernick, K. W. West, R. C. Sherwood, and G. Y. Chin, Phys. Rev. 188, 684 (1969).

[23]L. D. Roberts, R. L. Becker, F. E. Obenshain, and J. O. Thomson, Phys. Rev. 137, A895 (1965).

[24]L. D. Roberts and J. O. Thomson, Phys. Rev. 129, 664 (1963).

[25]J. Burton, J. O. Thomson, P. G. Huray, and L. D. Roberts (unpublished).

[26]P. G. Huray, L. D. Roberts, and J. O. Thomson, Bull. Am. Phys. Soc. 13, 667 (1968); P. G. Huray, thesis, University of Tennessee, 1968 (unpublished); P. G. Huray, L. D. Roberts, and J. O. Thomson, in *Hyperfine Structure and Nuclear Radiation*, edited by E. Matthias and D. A. Shirley (North-Holland, Amsterdam, 1968), p. 596.

[27]D. O. Patterson, J. O. Thomson, L. D. Roberts, R. G. Scurlock, and P. Lynam, Bull. Am. Phys. Soc. 11, 50 (1966).

[28]J. O. Thomson, P. G. Huray, D. O. Patterson, and L. D. Roberts, in *Hyperfine Structure and Nuclear Radiations*, edited by E. Matthias and D. A. Shirley (North-Holland, Amsterdam, 1968), p. 557; D. O. Patterson, thesis, University of Tennessee, 1966 unpublished .

[29]P. Lynam, W. Proctor, S. M. Puri, and R. G. Scurlock, following paper, Phys. Rev. 2, 2448 (1970).

[30]O. C. Kistner and A. W. Sunyar, Phys. Rev. Letters 4, 412 (1960); D. A. Shirley, Rev. Mod. Phys. 36, 339 (1964).

[31]L. D. Roberts, D. O. Patterson, J. O. Thomson, and R. P. Levey, Phys. Rev. 179, 656 (1969).

[32]From this value for B we have given an estimate of $\delta r_n/r_n$ of $+1.5\times10^{-4}$. Barrett *et al.* (Ref. 18) and Faltens (Ref. 20) have given values for $\delta r_n/r_n$ in the range from $+2$ to $+3\times10^{-4}$.

[33]H. Dahmen and S. Penselin, Z. Physik 200, 456 (1967).

[34]A. Bohr and V. F. Weisskopf, Phys. Rev. 77, 94 (1950).

[35]D. A. Shirley has called our attention to the fact that the hfs anomaly has been observed in atomic beam experiments for ^{197}Au and ^{198}Au [P. A. Vandenbout, V. J. Ehlers, W. A. Nierenberg, and H. A. Shugart, Phys. Rev. 158, 1078 (1967); P. A. Vandenbout, UCRL Report No. 16757, 1966 (unpublished)] and that it may be of importance in obtaining a value for μ^* from our measurements. This anomaly has been observed in Mössbauer studies for ^{193}Ir by Perlow *et al.* [G. J. Perlow, W. Henning, D. Olson, and G. L. Goodman, Phys. Rev. Letters 23, 680 (1969)].

[36]D. Seyboth, F. E. Obenshain, L. D. Roberts, and J. O. Thomson, Bull. Am. Phys. Soc. 10, 444 (1965).

[37]W. J. Childs and L. S. Goodman, Phys. Rev. 141, 176 (1966).

[38]P. M. Parker, J. Chem. Phys. 24, 1096 (1956).

[39]J. W. Burton, L. D. Roberts, and J. O. Thomson, Bull. Am. Phys. Soc. 13, 250 (1968).

[40]P. Steiner, E. Gerdau, W. Hautsch, and D. Steenken, in *Hyperfine Structure and Nuclear Radiations*, edited by E. Matthias and D. A. Shirley (North-Holland, Amsterdam, 1968), p. 364.

[41]W. C. Hamilton, *Statistics in Physical Science*

(Ronald Press, New York, 1964).
[42]S. V. Karyagin, Fiz. Tverd. Tela 8, 1739 (1966) [Soviet Phys. Solid State 8, 1387 (1966)].
[43]We are indebted to Dr. R. L. Cohen for pointing out that the line intensities ratios I_1/I_8, etc., depart slightly from unity when the magnetic axis is not parallel to that of the efg.
[44]M. Atoji, Phys. Letters 28A, 139 (1968).

PHYSICAL REVIEW B VOLUME 2, NUMBER 7 1 OCTOBER 1970

Hyperfine Fields at ^{55}Mn in Ordered Au-Mn Alloys from Low-Temperature Specific-Heat Measurements

P. Lynam, W. Proctor, S. M. Puri, * and R. G. Scurlock
Department of Physics, University of Southampton, S09 5NH, England
(Received 9 June 1969)

The specific heat of the ordered alloys AuMn, Au_2Mn, Au_3Mn, Au_4Mn, and $AuMn_3$ has been measured in the temperature range from 0.25 to 3.9 °K. In addition to the electronic, lattice, and nuclear Schottky contributions to the total specific heat, the results show an anomaly at temperatures below about 0.6 °K, the origin of which may be associated with magnetic ordering. The variation with composition of the hyperfine field is discussed in terms of the magnetic environment of the ^{55}Mn nucleus.

I. INTRODUCTION

The hyperfine field at the host nuclei in binary alloys of transition metals with nonmagnetic impurities is known to depend markedly on the magnetic environment. For this reason the study of hyperfine coupling in ordered alloys is very useful, because the magnetic environment of the host nuclei should be well defined. Alloys of manganese and gold form a suitable system for study by the specific-heat method, since five ordered phases, AuMn, Au_2Mn, Au_3Mn, Au_4Mn, and $AuMn_3$ are formed. Since the gold nuclei carry a magnetic moment of 0.144 86 μ_N, the total nuclear specific heat must be corrected for the contribution from the gold hyperfine interaction. Fortunately, ^{197}Au has a resonance γ ray suitable for Mössbauer effect measurements, thus enabling this correction to be made.

The hyperfine field at the ^{55}Mn nuclei in these five ordered Au-Mn alloys has been deduced from the results of specific-heat measurements made in the temperature range from 0.25 to 3.9 °K. The specific-heat results were corrected using the values of the hyperfine field at the gold nuclei as obtained by Patterson *et al.*[1] from Mössbauer measurements on samples from the same melts.

In addition to the T^{-2} contribution to the specific heat, arising from the nuclear hyperfine interaction, a further positive contribution was observed, and is discussed in a later section.

II. EXPERIMENTAL PROCEDURE AND RESULTS

Details of the preparation of the specimens and the annealing procedures for producing the ordered phases, together with the results of an x-ray analysis, are given by Patterson *et al.*[1] The specific-heat measurements were made initially in the temperature range from 0.25 to 1 °K, with an adiabatic demagnetization cryostat, but this range was later extended up to 3.9 °K by the use of a ^{3}He cryostat, which has been described elsewhere.[2] The results are plotted as specific heat C against temperature T in Fig. 1. There is good agreement between the two sets of results in the overlapping temperature region.

At temperatures below 4 °K the total specific heat of a normal ferro- or antiferromagnet can usually be represented by the equation

$$C = \gamma T + AT^3 + BT^{-2}, \quad (1)$$

where γ and A are the coefficients of the electronic and lattice specific-heat contributions, respectively, and B is the coefficient of the first term in the expansion of the nuclear Schottky specific heat. Spin-wave contributions have been omitted from the above expression because they are expected to be small and are difficult to separate from the lattice contribution in measurements below 4 °K. If the lattice contribution is subtracted from the total specific heat, and the remainder is plotted as CT^2 against T^3, a straight line should result.